

## Article

# Hybrid Energy Storage System Taking Advantage of Electric Vehicle Batteries for Recovering Regenerative Braking Energy in Railway Station

Hamed Jafari Kaleybar <sup>\*</sup>, Mostafa Golnargesi, Morris Brenna  and Dario Zaninelli

Energy Department, Politecnico di Milano, 20156 Milan, Italy; mostafa.golnargesi@mail.polimi.it (M.G.); morris.brenna@polimi.it (M.B.); dario.zaninelli@polimi.it (D.Z.)

\* Correspondence: hamed.jafari@polimi.it

**Abstract:** Nowadays, nations are moving toward the electrification of the transportation section, and the widespread development of EV charging stations and their infrastructures supplied by the grid would strain the power grid and lead to overload issues in the network. To address this challenge, this paper presents a method for utilizing the braking energy of trains in railway stations to charge EVs located in strategic areas like park-and-ride regions close to railway stations improving energy efficiency and preventing grid overload. To validate the feasibility of the proposed system, a metro substation in Milan city is considered as a case study located in outskirts of the city and contains large number of parking space for vehicles. Three different scenarios are evaluated including DC fast charging station, AC low charging station and collaborative hybrid energy storage based AC charging station as EV charging station type. The results are studied for different EV population number, charging rate and the contractual power grid. Meanwhile, the possibility of proposed system in participating as V2G technology and taking advantage of the EV's batteries to provide ancillary support to accelerating trains is investigated regarding peak shaving objective. The results indicated that the suggested interconnected system operates effectively when a significant quantity of EVs are parked at the station. However, the results revealed that the performance of the proposed system is notably influenced by other factors and a limited number of EVs during the early morning and late evening periods. Overall, this study confirms the feasibility of energy transfer between two types of transportation means in intermodal areas.

**Keywords:** electric vehicle; electric railway; regenerative braking energy; charging station; traction substation; hybrid energy storage system



**Citation:** Jafari Kaleybar, H.; Golnargesi, M.; Brenna, M.; Zaninelli, D. Hybrid Energy Storage System Taking Advantage of Electric Vehicle Batteries for Recovering Regenerative Braking Energy in Railway Station. *Energies* **2023**, *16*, 5117. <https://doi.org/10.3390/en16135117>

Academic Editor: Djaffar Ould-Abdeslam

Received: 20 April 2023

Revised: 21 June 2023

Accepted: 26 June 2023

Published: 2 July 2023



**Copyright:** © 2023 by the authors. Licensee MDPI, Basel, Switzerland. This article is an open access article distributed under the terms and conditions of the Creative Commons Attribution (CC BY) license (<https://creativecommons.org/licenses/by/4.0/>).

## 1. Introduction

The eagerness to decrease our reliance on fossil fuels and the negative effects that human transportation has on the environment have spurred substantial advancements in electrical transportation in recent years. A significant portion of the world's energy consumption, roughly 36%, is accounted for by the transportation sector, according to International Energy Agency (IEA) members [1]. The move away from burning fossil fuel is increasing overall electricity demand, and the unchecked charging of an electrical transportation system that is constantly evolving results in power demand peaks that run the risk of overloading local distribution grid.

Despite the integration of renewable energy sources (RESs) to supply EV charging station (EVCS) being widely reviewed in the literature [2–5], adopting the intrinsically produced braking energy of trains reaching stations to supply of EVCSs has not been evaluated much. However, several solutions have been put forth to maximize the reuse of recovered braking energy (RBE): train timetable optimization, investigating the synchronization of many trains and optimizing train timetables; energy storage systems (ESS) and reversible substations [6–9].

Despite many publications regarding these utilization methods, a few papers have paid attention to charge EVs directly from RBE. In [10,11] studies have been conducted regarding the amount of lost RBE in metro system and the possibility of charging EVs with such a wasted energy. In [12,13] a cost optimization method is presented for a shared microgrid based on RES, railway system and EV parking station. In this regard, the integration architectures are presented as different scenarios as smart ERSs [14,15]. However, the possibility of transferring RBE into EVs is not evaluated in these research. In other words, the direct transmission of RBE from train into EVs batteries is a main challenge because of high difference in the range of power produced by a braking train and power needed by EVs.

The high-power DC fast charging technologies can be a promising option to be interconnected to railway station enhancing the power absorption potential of EVCS [16]. However, the implementation of numerous DC fast charging technologies in park-and-ride regions would be very expensive and might not have any economic justification.

In [17,18], modified control methods are presented to charge EVs from high-speed railway systems taking advantages of back-to-back converters and internal ESSs. In this situation, ESS may also cooperate in decreasing peak power demand pressures on the utility grid that are brought on by power requirements of trains, especially during acceleration when motoring power may exceed a few megawatts depending on the railway network type. However, this system has been proposed for high-speed railway substation that transfer RBE from AC side to charge EVs.

Motivated by aforementioned challenges, this paper evaluate the possibility of integrating AC and DC EVCSs into the DC metro railway system inside urban and park-and-ride areas by presenting a concept of V2G. V2G concept in this regard, in contrast to other ESS, makes use of storage that would otherwise be unused (batteries of parked EVs). Existing EV batteries are given a secondary use rather than producing and maintaining specialized energy storage systems for electric trains systems. The combined EV population can either be discharged to help adjacent accelerating trains, decreasing peak power demand of substation, or charged by absorbing power from RBE. The population of EVs can use the joint connection to the utility for charging if there are no adjacent trains.

In [19], it is shown that the dependence on the availability of EVs in sufficient quantities is the main drawback of V2G in comparison to other ESS. They have studied the EVs to manage the braking and acceleration energy without using the extra energy storage device, and charging rate is considered to be at least 20 kW, which shows the DC charging method.

In this paper, taking advantage of internal hybrid energy storage system, the suitable charging rate has been decreased to 6 kW, which confirms the possibility of direct charging of EVs with even AC chargers. The weighting management-based method in EV aggregator section is proposed so that each EVs according to its SOC can participate in the absorption of RBE or supplying train in accelerating mode. In other words, the main idea of this paper is to show the feasibility of integrating railway substation and EV charging station and charging EV battery with wasted braking energy of trains. The main challenge of this integration is the power compatibility in both sides. In other words, the trains' power are in the range of several MW, while EVs' power are in the range of several kW. Overall, the prominent contributions presented in this paper can be listed as:

- Confirming the feasibility of integrating railway substation and EV charging station to charge EV battery with wasted braking energy of trains;
- Proposing HESS as a buffer making the power ranges compatible in both sides;
- Studying the effects of crucial factors in the proposed integration system, which varies based on the type of charging technology employed.

Simulation results based on 24 h profile considering a single train movement together with braking and acceleration events are provided to verify the above-mentioned goals. Therein, the size of the HESS is fixed, and the EV population size and the overall power made available from the power grid are considered as variables.

The rest of the paper is structured as follows. Section 2 is dedicated to the modeling of the proposed system containing ERSs, hybrid energy storage system and EV charging station. Then, in Section 3, the proposed power charging management system for aggregator is presented. Section 4 demonstrates the simulation results of various scenarios and analysis for the considered case study with AC and DC fast charging systems. Finally, Section 5 concludes the paper.

## 2. Principles of Proposed System

### 2.1. Electric Railway System Modeling

The general layout of the proposed system is depicted in Figure 1. It is considered that a charging station for electric vehicles (EVCI) connected to the grid is situated at a traction substation (TSS) in a park-and-ride area that has over 400 empty parking spaces. For the purpose of this study, the San Donato station in Milan is used as a practical example. The TSS converts AC to 1500 V DC taking advantage of 12 pulse rectifiers [20]. The daily train traffic in the station is taken into account, including both instances of acceleration and braking for one train, based on an analysis of the daily profile of the park-and-ride area. In semi-rush hours, the power profile for TSS over a one-hour period is shown in Figure 2a. A maximum power demand of 1.15 MW is expected for metro locomotives, and a contracted power known as the grid connection limit is necessary to provide a continuous supply of power to the substation due to this power range and the TSS's internal loads. As illustrated in the figure, the anticipated profile for the substation is deemed almost ideal under normal railway operation conditions (variations in train weight, passenger numbers and the exact moments of train arrival and departure are not taken into account). The 24 h power profile model for a weekend day indicates 117 train departures/arrivals. Around 4 h (16% of the day) are dedicated to the traction power needs for acceleration, while roughly 2 h (9%) are reserved for regenerative braking power, which can charge electric vehicle charging stations.

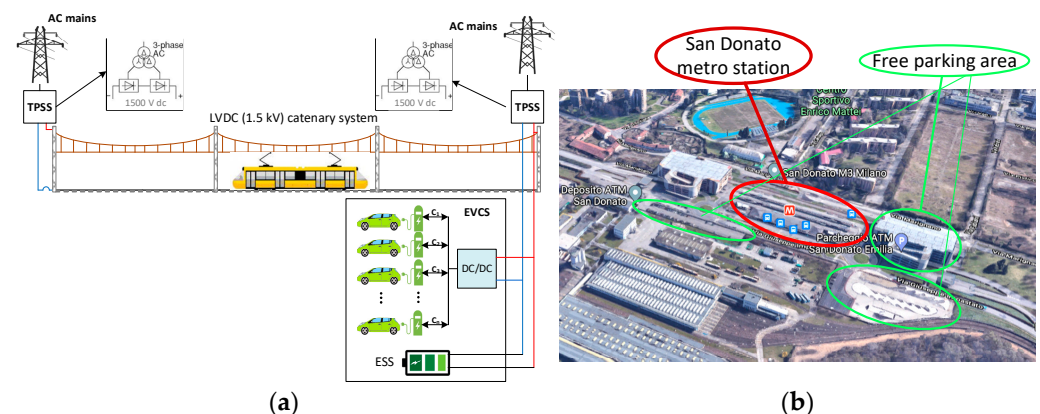


**Figure 1.** Proposed model of railway system and EVCS. (a) Schematic of the proposed railway and EVCS integrated system in park-and-ride area. (b) integrated system in park-and-ride area.

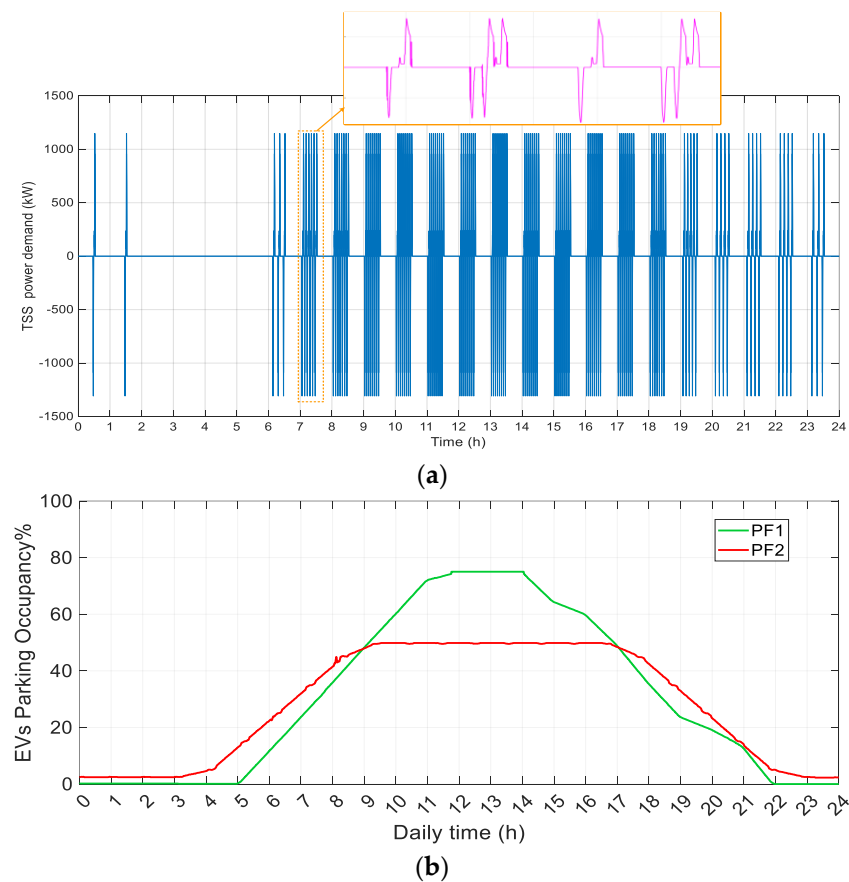


**Figure 2.** The power demand of TSS for one train and park-and-ride area occupancy. (a) Daily profile of TSS regarding consumed and generated power of one train. (b) Parking occupancy profiles for two different premises.

### 2.2. EV Charging Parking Lot Modeling

As previously mentioned, integrating electric vehicle charging infrastructure with metro railway systems requires consideration of the power disparity between the two systems (trains operate in the megawatt range, while EVs operate in the kilowatt range). High-power DC EV chargers or large AC EV charging stations with multiple low-power chargers are ideal choices for integration. To achieve this, a parking lot with over 400 parking spaces is proposed for integration, with 200 of these spaces equipped with AC EV charger (mode 3) technology. The proposed EV charging infrastructure will be linked to the DC hub of the metro railway system via a DC/AC converter. The converter will be controlled by an aggregator management system that takes into account the number of available EVs, their state of charge, and the maximum charging/discharging power. To design the parking lot and the substation of the railway system, the actual distribution profile that outlines the number of EVs throughout the day, as well as their arrival and departure times, must be established. Two power profiles related to big parking lots in such areas is shown in Figure 2b.

### 2.3. Hybrid Energy Storage System

Hybrid energy storage systems (HESSs) are becoming increasingly popular in railway systems due to their ability to reduce energy consumption, increase efficiency and improve reliability. However, determining the optimal size of a hybrid ESS for a railway system can be a challenging task as it requires consideration of several factors such as the type of trains, the operating conditions, and the power requirements [21–23]. To size a hybrid ESS for a railway system, the first step is to evaluate the power demand profile of the system. This

involves analyzing the power consumption patterns of the trains over a typical operating day or week, which can vary depending on factors such as the train schedule, the number of passengers, and the terrain. This data can be used to determine the average and peak power requirements of the system.

Considering the proposed system, when the train is in acceleration mode, the train power is larger than zero, and conversely, train power is sent back to the grid from the train in regenerative braking mode. As the substation required power exceeds the threshold region, first the power flow of EVs in the park-and-ride is responsible for peak shaving or valley filling. However, during the whole day, it cannot supply the total train power, so in the proposed method if the load power exceeds the power capacity of EVs, the HESS is in charge of supplying the remaining load power and vice versa.

A HESS main idea is that heterogeneous ESSs have complimentary qualities, particularly in terms of power and energy density. Instead of adopting only one kind of ESS, hybridization combines the benefits of both to offer better performance. An HESS is typically the combination of at least two ESS devices, one dedicated for high energy requirement and one for high power requirement, in railway applications. While the high-power device can be utilized as a supplier to fulfill short-term high-power demands, the high-energy set can be utilized as an energy supplier to meet long-term energy needs. To address the energy needs of rail systems, batteries and supercapacitor are ESS components that can be combined with a HESS.

The sizing of HESS for the proposed system is carried out based on defining threshold values for charging ( $P_{L1}$ ) and discharging ( $P_{L2}$ ) powers and the powers estimated by EV charging station aggregator. Accordingly,  $P_{ch\_t}$  and  $P_{dch\_t}$  also must be monitored and are available charging and discharging powers of EV charging station used to build the power allocation scale.

HESS is set up to discharge if the traction power is larger than  $P_{L1}$ . If the regenerated power is larger than  $P_{L2}$ , HESS is charging. Sometimes, the HESS is in offline mode. The following formulas can be used to state it precisely:

$$P_{HESS}(t) = \begin{cases} P_{load} - P_{dch\_t} & P_{load} > P_{L1} & \text{high power acceleration} \\ 0 & P_{L1} < P_{load} < P_{L2} & \text{offline mode} \\ P_{load} + P_{ch\_t} & P_{load} < P_{L2} & \text{high power braking} \end{cases} \quad (1)$$

### 3. Aggregation Control and Charging Management System

In the proposed EV parking lot, the connected EV population would discharge into the rail system as electric trains speed up, generating a rise in the power demand for traction and reducing the load on the nearby substation. When trains slow down using regenerative braking, the sudden increase in power generated by the rail system can be directed towards the EV parking lot. But, as EV parking lot is not able to supply whole power demand from train especially in the early morning and evening, hybrid energy storage system (HESS) is employed to mitigate power demand from the grid. In order to manage the energy exchange, the load profile has been categorized into three separate scenarios (events): (1) train departure event, which involves acceleration from a stationary position, slow movement near the station, and then travelling at a constant speed, requiring traction power; (2) train arrival event, which involves deceleration from travelling speed to a stop, with the energy generated from regenerative braking needing to be released; and (3) no traffic when there is no departure event or arrival event.

The EV parking lot is assumed to utilize the same substation and share its power grid connection as the train system (see Figure 1). It makes an effort to maintain the grid connection limit, or the power output from this substation remains constant, but it is not a strict limitation. Instead, it is a flexible constraint that is determined by the portion of available power that needs to be regulated by the EV parking lot. The aggregator continuously analyzes EVs and uses a dual-scoring system to rate them according to their suitability for consuming or supplying power. DCW and CW are the dual scores [13].

Charge Weighting (CW): An unsigned float value measuring how well the electric vehicle (EV) is suited to receive power (the greater the value, the more likely it will be used for charging). When SOC of EV battery reaches 90%, value is zero, and an EV can no longer be charged.

Discharge Weighting (DCW): An unsigned float value indicating how well-suited the EV is to provide power (the probability of an EV being selected for discharging is greater when its corresponding value is higher). Value is zero when SOC is lower than 10%, making it unable to discharge an EV any further.

In order to calculate the DCW and CW index, it is necessary to calculate state of charge (SOC) of every battery of EV parking lot and HESS. The mathematical model of state of charge for every EV, battery and supercapacitor are shown in Equations (2)–(4). SOC represents the ratio of energy store to capacity of EV, battery and supercapacitor.

$$S_{EV}^t = S_{EV}^1 + \frac{\sum_{t=1}^T P_{EVcha}^t \times \eta_{EV} \times C_{EV}^t \times t - \sum_{t=1}^T \frac{P_{EVdis}^t}{\eta_{EV}} \times D_{EV}^t \times t}{E_{EV}} \quad (2)$$

$$S_{Bat}^t = S_{Bat}^1 + \frac{\sum_{t=1}^T P_{Batcha}^t \times \eta_{EV} \times C_{EV}^t \times t - \sum_{t=1}^T \frac{P_{EVdis}^t}{\eta_{EV}} \times D_{EV}^t \times t}{E_{Bat}} \quad (3)$$

$$S_{SC}^t = S_{SC}^1 + \frac{\sum_{t=1}^T P_{SCcha}^t \times \eta_{SC} \times C_{SC}^t \times t - \sum_{t=1}^T \frac{P_{SCdis}^t}{\eta_{SC}} \times D_{SC}^t \times t}{E_{SC}} \quad (4)$$

where,  $t$  is the duration of charging or discharging,  $S_{EV}^t$ ,  $S_{Bat}^t$ ,  $S_{SC}^t$  are the SOC of EV, battery and supercapacitor, respectively.  $S_{EV}^1$ ,  $S_{Bat}^1$ ,  $S_{SC}^1$  are the initial values of the state of the charge SOC of EV, battery and supercapacitor, respectively. The  $C_{EV}^t$  and  $D_{EV}^t$  are the charging and discharging state of EV, respectively. Similarly,  $C_{Bat}^t$ ,  $D_{Bat}^t$  and  $C_{SC}^t$ ,  $D_{SC}^t$  are charging and discharging state of battery and supercapacitor and  $P_{EVcha}^t$  and  $P_{EVdis}^t$  are the charging and discharging state of EV and  $P_{Batcha}^t$ ,  $P_{Batdis}^t$  and  $P_{SCcha}^t$ ,  $P_{SCdis}^t$  are the charging and discharging power of battery and supercapacitor, respectively. When activated, charging will add to the amount of power stored in the EV, while discharging will decrease the stored power. It is important to note that the EV can only be in one state of either charging or discharging at a given time, so  $C_{EV}^t$ ,  $C_{Bat}^t$ ,  $C_{SC}^t$  and  $D_{EV}^t$ ,  $D_{Bat}^t$ ,  $D_{SC}^t$  are dedicated to the charging and discharging state of the EV, battery and supercapacitor, respectively, and their values can be 0 or 1, where they cannot be 1 at the same time. When  $C_{EV}^t$ ,  $C_{Bat}^t$ ,  $C_{SC}^t$  is 1, the first part of the equation represents the enhancement of electricity. When  $D_{Bat}^t$ ,  $D_{Bat}^t$ ,  $D_{SC}^t$  is 1, the second part of the equation indicates the reduction in electricity at a specific time,  $t$ . To determine the change in electricity stored from the initial time, the total amount of charging and discharging electricity up to time  $t$  needs to be added up. This applies to all EVs, batteries and supercapacitors.

The EV, battery and supercapacitors' charging and discharging efficiencies, respectively, can be calculated as follow [24]:

$$\eta_{EVchar} = \eta_{EVchar}^{ess} \times \eta_{DC/DC} \times \eta_{DC/AC} \quad (5)$$

$$\eta_{EVdis} = \eta_{EVdis}^{ess} \times \eta_{DC/DC} \times \eta_{DC/AC} \quad (6)$$

$$\eta_{Batchar} = \eta_{Batchar}^{ess} \times \eta_{DC/DC} \times \eta_{DC/AC} \quad (7)$$

$$\eta_{Batdis} = \eta_{Batdis}^{ess} \times \eta_{DC/DC} \times \eta_{DC/AC} \quad (8)$$

$$\eta_{SCchar} = \eta_{SCchar}^{ess} \times \eta_{DC/DC} \times \eta_{DC/AC} \quad (9)$$

$$\eta_{SCdis} = \eta_{SCdis}^{ess} \times \eta_{DC/DC} \times \eta_{DC/AC} \quad (10)$$

The charging and discharging efficiencies of EV, battery and supercapacitor themselves are represented in Equations (5)–(10) by  $\eta_{EVchar}$ ,  $\eta_{Batchar}$ ,  $\eta_{SCchar}$  and  $\eta_{EVdis}$ ,  $\eta_{Batdis}$ , respectively. Efficiency of a DC/DC converter is expressed as  $\eta_{DC/DC}$  and that of a DC/AC converter as  $\eta_{DC/AC}$ .

When the SOC of each EV, battery and supercapacitor are calculated, the methods used to calculate their CW and DCW values vary depending on the specific use case. In cases where power needs to be supplied to the EV station, EVs are deemed more valuable to the aggregator if their battery has a high capacity, a low state of charge SOC and a high maximum charging rate. Conversely, when power needs to be drawn from the EV station, EVs are more valuable if their batteries have a higher capacity, a higher SOC and a higher maximum discharging rate. Therefore, charge weighting and discharge weighting can be defined as follows:

$$CW_i = (1 - SOC_i) \times \frac{C_i}{C_b} \times \frac{P_{Ch-max}}{P_{Ch-b}} \quad (11)$$

$$DCW_i = SOC_i \times \frac{C_i}{C_b} \times \frac{P_{Ch-max}}{P_{Ch-b}} \quad (12)$$

where,  $C_b$  is base capacity, and  $P_{Ch-b}$  is base power rating. The EV population can use the shared grid link to draw electricity during times when there is no rail traffic, maintaining a constant power flow from the system. The EV population uses the shared grid connection for smart charging when there is no train activity. Every electric vehicle (EV) is allocated a minimum power ( $P_{min}$ ) and a portion of the remaining power ( $P_{Rm}$ ), which is dependent on its ranking. This power together with shared power can be calculated as (13) and (14).

$$P_{Rm} = P_{Gr} - \sum_{i=1}^n P_{min} \quad (13)$$

$$P_{sh} = \frac{P_{Rm}}{\sum_{i=1}^n CW_i} \quad (14)$$

where  $P_{Gr}$  is grid power, and  $P_{sh}$  is the share power, which is allocated to every EV based on its rank. The rank of every EV is evaluated with Equation (11). Accordingly, power demand ( $P_{Dem}$ ) of every EV is calculated based on Equation (15).

$$P_{Dem} = CW_i \cdot P_{sh} \quad (15)$$

If the power demand would be greater than maximum charging rate of EV, the power demand is equal to maximum charging rate; otherwise, EV absorbs power corresponding to the its power demand, and the extra power is stored in battery and supercapacitor.

The battery pack SOC at the time determines the maximum charging rate for each EV. So, regardless of the battery pack SOC, it is a logical assumption to make that the battery pack can be discharged at least at this rate. The estimated charging/discharging limits of any bi-directional EV charger are exceeded by this discharging rate.

For train departure events, the aggregator switches grid connection power from EVs to train. Then, aggregator for supplying the traction power priorities EVs that have a high battery capacity, a high maximum discharging rate and a high SOC and are considered valuable in the scoring system, with each parameter carrying equal weight. These EVs are particularly useful during train departures as they can provide a significant amount of energy in a shorter amount of time compared to the rest of the EV population. Finally, if the power store in the EV parking lot cannot supply the traction power, HESS that consists

of supercapacitor and battery is in charge of covering the remain traction power. If the power discharged by the supercapacitors is inadequate to match the power demand of the system, the battery is utilized to discharge energy. If Equation (16) is true during the whole acceleration event, the aggregator does not demand power from the grid. The primary aim is to reduce the energy consumption from the grid network. Therefore, if aggregate meet Equation (16), we achieve our aim. However, if during part of the acceleration event, Equation (16) is not true, the remaining power must be obtained from the grid, and this situation is not satisfactory.

$$P_{Grid\ Connection}^t + P_{EVs}^t + P_{Badis}^t + P_{SCdis}^t \geq P_{train}^t \tag{16}$$

where,  $P_{Grid\ connection}^t$  is the constant power, which is obtained from the power network,  $P_{EVs}^t$  is the power provision by the EVs,  $P_{Badis}^t$  and  $P_{SCdis}^t$  are the power provisions by the battery and supercapacitor of HESS, respectively, and  $P_{train}^t$  is the power absorption by train in the traction mode (acceleration).

In Equations (17)–(19), constraints conditions for EV, battery and supercapacitor are explained to avoid occurrence of overcharging or over-discharging. Additionally, there are limitations on the power range for charging or discharging, and EVs can only be charged or discharged at a specific time.

$$\left\{ \begin{array}{l} S_{EV}^{min} \leq S_{EV}^t \leq S_{EV}^{max} \\ S_{EV}^1 = S_{EV}^T \\ 0 \leq C_{EV}^t + D_{EV}^t \leq 1 \\ C_{EV}^t \in \{0, 1\} \\ D_{EV}^t \in \{0, 1\} \\ 0 \leq P_{EVcha}^t \leq P_{EVcha}^{max} \\ 0 \leq P_{EVdis}^t \leq P_{EVdis}^{max} \end{array} \right. \tag{17}$$

$$\left\{ \begin{array}{l} S_{Bat}^{min} \leq S_{Bat}^t \leq S_{Bat}^{max} \\ S_{Bat}^1 = S_{Bat}^T \\ 0 \leq C_{Bat}^t + D_{Bat}^t \leq 1 \\ C_{Bat}^t \in \{0, 1\} \\ D_{Bat}^t \in \{0, 1\} \\ 0 \leq P_{Batcha}^t \leq P_{Batcha}^{max} \\ 0 \leq P_{Batdis}^t \leq P_{Batdis}^{max} \end{array} \right. \tag{18}$$

$$\left\{ \begin{array}{l} S_{SC}^{min} \leq S_{SC}^t \leq S_{SC}^{max} \\ S_{SC}^1 = S_{SC}^T \\ 0 \leq C_{SC}^t + D_{SC}^t \leq 1 \\ C_{SC}^t \in \{0, 1\} \\ D_{SC}^t \in \{0, 1\} \\ 0 \leq P_{SCcha}^t \leq P_{SCcha}^{max} \\ 0 \leq P_{SCdis}^t \leq P_{SCdis}^{max} \end{array} \right. \tag{19}$$

where,  $S_{EV}^t, S_{Bat}^t, S_{SC}^t$  are the SOC of EV, battery and supercapacitor, respectively.  $S_{EV}^1, S_{Bat}^1, S_{SC}^1$  are the initial values of the state of the charge SOC of EV, battery and supercapacitor, respectively. To simplify the scheduling of the next working day, the initial SOC of supercapacitors must be same as the final SOC ( $S_{SC}^T, S_{Bat}^T$ ). The  $C_{EV}^t, D_{EV}^t, C_{Bat}^t, D_{Bat}^t, C_{SC}^t, D_{SC}^t$  are the charging and discharging state of EV, battery and supercapacitor, respectively. Meanwhile,  $P_{EVcha}^t, P_{EVdis}^t, P_{Batcha}^t, P_{Batdis}^t, P_{SCcha}^t, P_{SCdis}^t$  are the charging and discharging power of EV, battery and supercapacitor, respectively. It is important to note that the EV can only be in one state, of either charging or discharging, at a given time, so  $C_{EV}^t, C_{Bat}^t, C_{SC}^t$  and  $D_{EV}^t, D_{Bat}^t, D_{SC}^t$  are introduced to represent the charging and discharging state of the EV, battery and supercapacitor, respectively, and their amounts can take the value of 0 or 1 [24]. The proposed CW and DCW based charging management system flowchart

for G2V (flowing energy from trains to EVs) and V2G mode (flowing energy from EVs to trains) is illustrated in Figure 3.

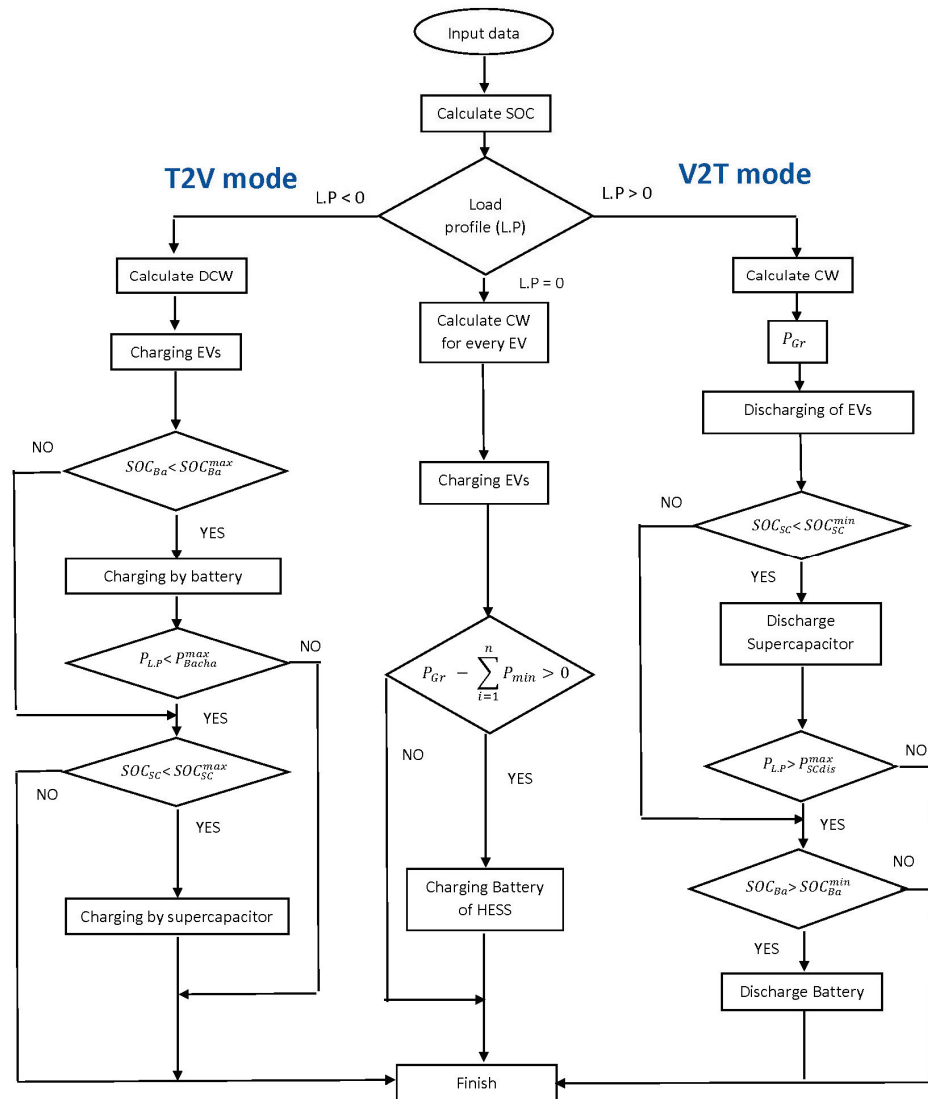
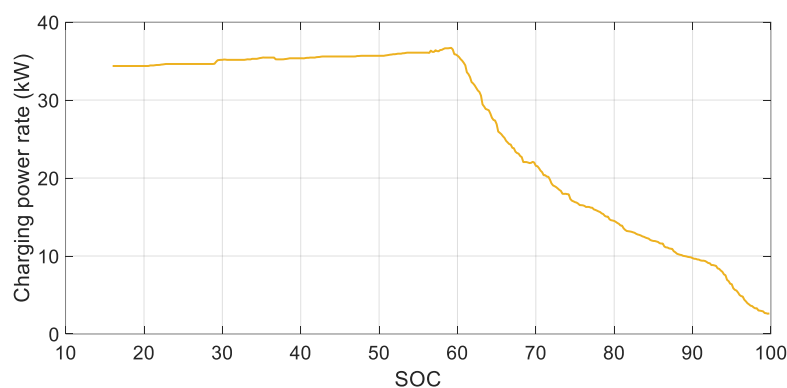


Figure 3. The proposed CW and DCW based charging management system flowchart.

On the other hand, during the braking event, aggregator confronts two energy sources, first grid connection power and regenerative braking power. In order to manage these two energy source, firstly, aggregator share grid connection power between EVs. Based on the proposed algorithm, EVs that have a high capacity, a high maximum charging rate (at that specific time) and a low SOC are given priority. Compared to the rest of the EV population, these EVs have the ability to rapidly store a significant amount of electrical energy. Then, if whole grid connection power is shared between EVs and still there is vacant space in the battery of EVs (based on the charging profile shown in Figure 4), regenerative braking energy fill the vacant space of the EV battery to charge the EVs with maximum rate. After that, HESS is in the charging state, with the batteries being the first to activate. If the regenerative braking power exceeds the maximum charging power of the batteries, the supercapacitors are also activated for charging simultaneously to absorb the regenerative braking power.



**Figure 4.** A typical charging profile for EV with DC fast charging system.

#### 4. Simulation and Results

In order to verify the proposed system and evaluate the optimum parameter required for each cases of AC or DC fast charging system, MATLAB software-based analyses are carried out in three different scenarios. The aggregator assigns EVs in a sequential manner to charge or discharge at the fastest rate possible during events, continuing to do so while the power absorbed from the substation reaches the predetermined limit for grid connection. The capacity of the EV population, the maximum charging and discharging rates of each EV as allowed by the aggregator and the expected limit for grid connection all play a crucial role in determining whether the V2G network can separate the power requirement of the railway network from the power network or not.

It is important to note that it is preferable to clarify the simulation's parameters before assessing the report's findings. The parameters are all given in Table 1. The first row relates to the HESS's specifications. There is an ESS that works with traction power and can hold RBE. Additionally, 0.95 is assumed as the efficiency of the DC–DC and AC–AC converters at the EV parking area. Furthermore, it is considered that there are three different scenarios for charging the EV (20 kW, 6 kW and 6 kW + HESS), and Table 1 lists the technical characteristics of the EVs, including a typical EV DC fast charging profile shown in Figure 4. Each of scenarios are studied based on three modes of EV populations including 75, 100 and 150 EVs. The term 20 kW, which is used in scenario 1, is the average charging power rate of this profile, demonstrating the general range for currently prevalent Mode 4 charging system. The primary objective is to highlight the distinctions between low-level AC charging systems and DC fast charging systems effects on the proposed integration system. With this focus in mind, we have opted to present an average value for the currently prevalent Mode 4 charging system in Scenario 1. Furthermore, it is obvious that the charging profile for AC systems remains relatively consistent among various car models. The parameters of the load profile and the corresponding power demand curve are shown in Table 1.

**Table 1.** Parameters of the proposed system.

	Parameters	Value
HESS	Battery charging rate	$55 \times 6 \text{ kW} \text{—}(330 \text{ kW})$
	Battery capacity	440 Ah
	Supercapacitor charging rate	100 kW
	Supercapacitor capacity	4000 kJ
Load profile	Nominal traction power of train	1009 kW
	Nominal braking power of train	1109 kW
EV station	DC fast charging rate	20 kW
	EV battery capacity	40 kWh
	AC charging rate	6 kW

#### 4.1. Scenario 1: Charging Rate 20 kW-DC Fast Charger

To investigate this scenario, a simulation of the 24 h system operation is conducted, considering three different EV populations consisting of up to 150, 100 and 75 EVs, respectively, with the grid connection limit and the maximum global charging rate per EV remaining constant at an average value of 20 kW from Figure 3 and 200 kW, respectively. In each of the three scenarios, the potential provision power output for the V2G network is depicted in Figure 5. If the power supply potential surpasses the threshold of approximately 1109 kW (which is equivalent to the peak power demand during a train departure event), the V2G network is deemed capable of completely powering such an event, resulting in a maximum reduction in peak power demand experienced by the utility grid. Accordingly, the V2G network is assumed to be capable of completely supplying a train acceleration in this scenario. As seen in the figure, all three scenarios exceed this threshold from ~08:30 to ~19:30.

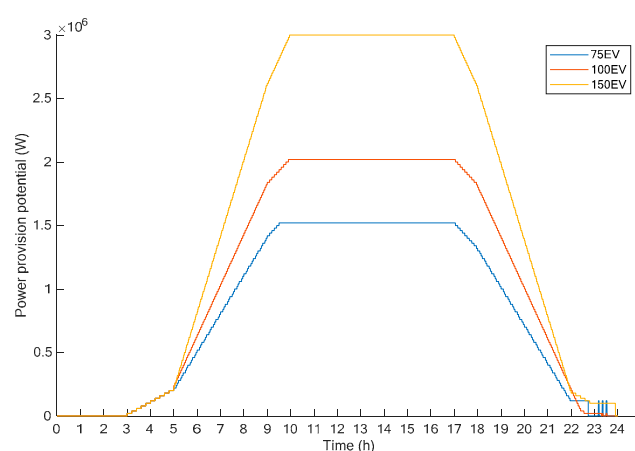


**Figure 5.** Total power provision potential of EV charging station with different numbers for scenario 1 (20 kW).

The diagrams in Figure 5 demonstrate how the power supply potential of EVs have the potential to lessen the peak power requirements of a substation. Figure 6a illustrates the original power demands of the substation for train traction power for 75 EVs. Figure 6b shows the specified conditions of 100 EVs. The results confirm that the use of a V2G network and supplying train with EV batteries results in a decrease in the peak power demand. However, it is obvious that for 75 EVs, in the morning, there are still some peaks absorbed from substation.

Figure 7 illustrates the capability of the proposed network to receive regenerative power at various time points, with the total being the maximum charging rate of all EVs at that moment and restricted to a global charging limit of 20 kW. The highest power that an EV can receive for charging is based on its current state of charge (SOC), as shown in Figure 4. As shown in Figure 7, this threshold is never surpassed in the mode of EV population up to 75 EVs. The V2G network can solely accommodate regenerative braking energy for an extended duration in mode 1 and 2, which involve up to 150 EVs (from approximately 7:00 to 18:00, encompassing 85 of the 117 train arrivals, i.e., around 73%).

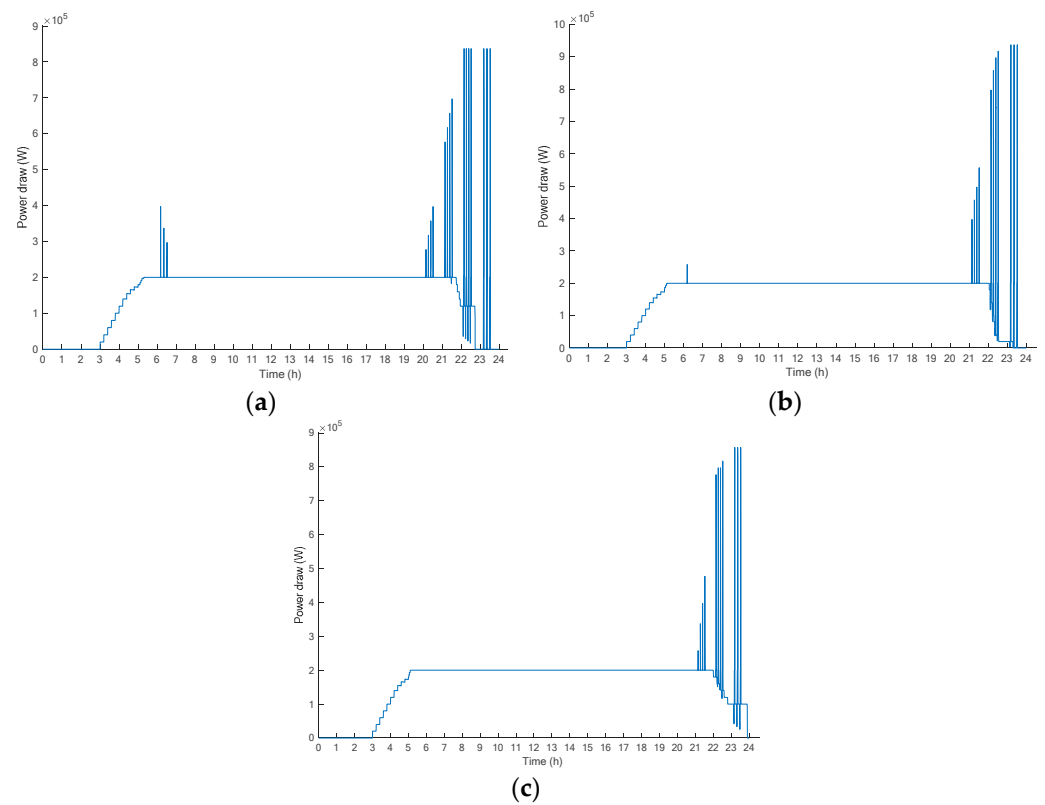


**Figure 6.** The power consumed by the rail system from the substation and the power demands of the EV population with a connected V2G network were recorded for scenario 1 (20 kW)—(a) 75 EVs. (b) 100 EVs. (c) 150 EVs.

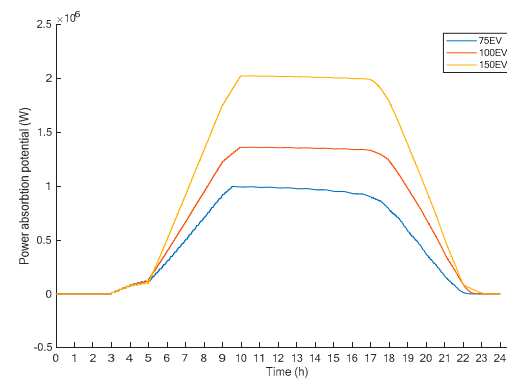


**Figure 7.** The total potential for power absorption of EV charging station with different numbers for scenario 1.

To reveal the effectiveness of proposed energy management system and to show that even after participating in the V2G scenario the EV batteries are charged when leaving the parking lot, Figure 8 illustrates evolution of the state of charge (SOC) for the three populations of EVs in each of the three scenarios (75, 100 and 150 EVs) considering initial SOC as 40% and 60%. The initial SOC of each simulated EV in reality is random; however, this work uses this assumption to simplify the analysis and provide initial insights. Assuming consistent SOC levels, it is possible to explore the fundamental principles and underlying mechanisms of the proposed system and integration.

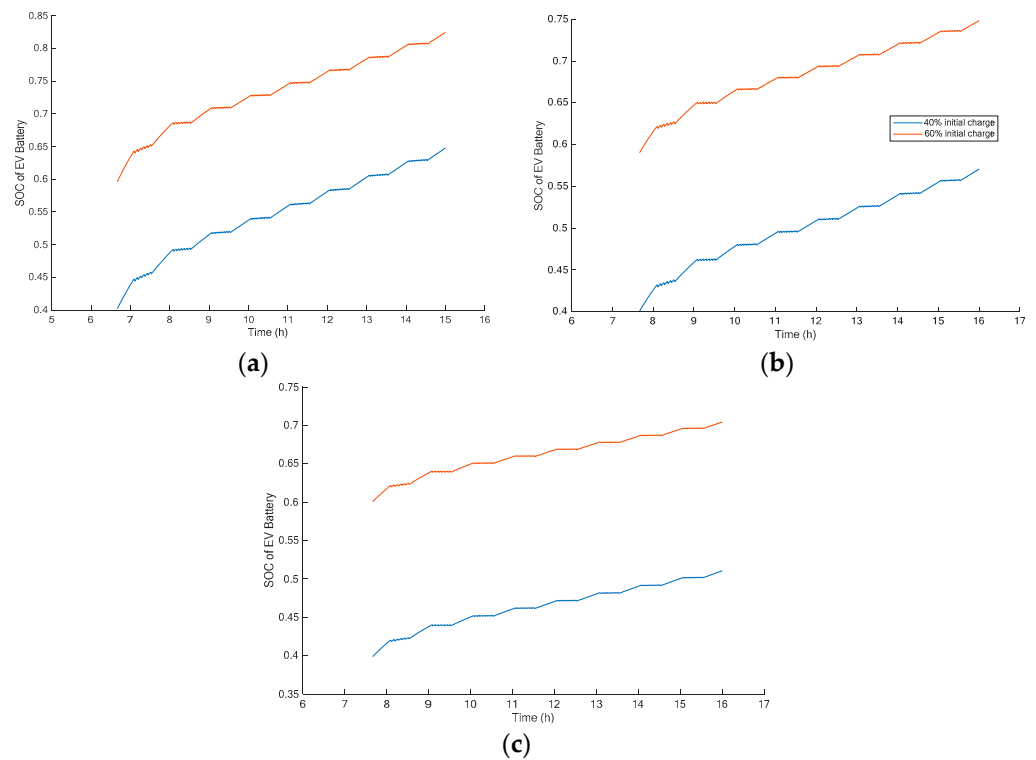


**Figure 8.** Changes in SOC over time of EVs (20 kW)—(a) 75 EVs. (b) 100 EVs. (c) 150 EVs.

The numerical values of SOC are presented for each EV number in Table 2. It is confirmed that even after participating in V2G, in all three scenarios, each EV SOC has a significantly increased leaving average of 22%. The results also reveal that with high number of EVs in the parking lot, the slope of charging is lower.

**Table 2.** The battery pack state of charge (SOC) of the control EVs with different EV population sizes for 20 kW scenario.

Initial Charge	Final Charge		
	75 EV	100 EV	150 EV
40%	66	61	57
60%	86	79	75

To analyze grid connection aspects, the researchers conducted multiple simulations of 24 h system operation with different grid connection limits, ranging from 100 to 400 kW. The EV population size remained constant at 75, 100 and 150 EVs for all simulations. The results are demonstrated in Figure 9. While the power demand of the rail system remains unchanged across scenarios, an increase in the power made available to the system leads to faster gains in SOC for connected EVs due to increased charging rates. Also, it is obvious that by increasing the grid connection power limit, the capability of regenerative braking power is decreased.

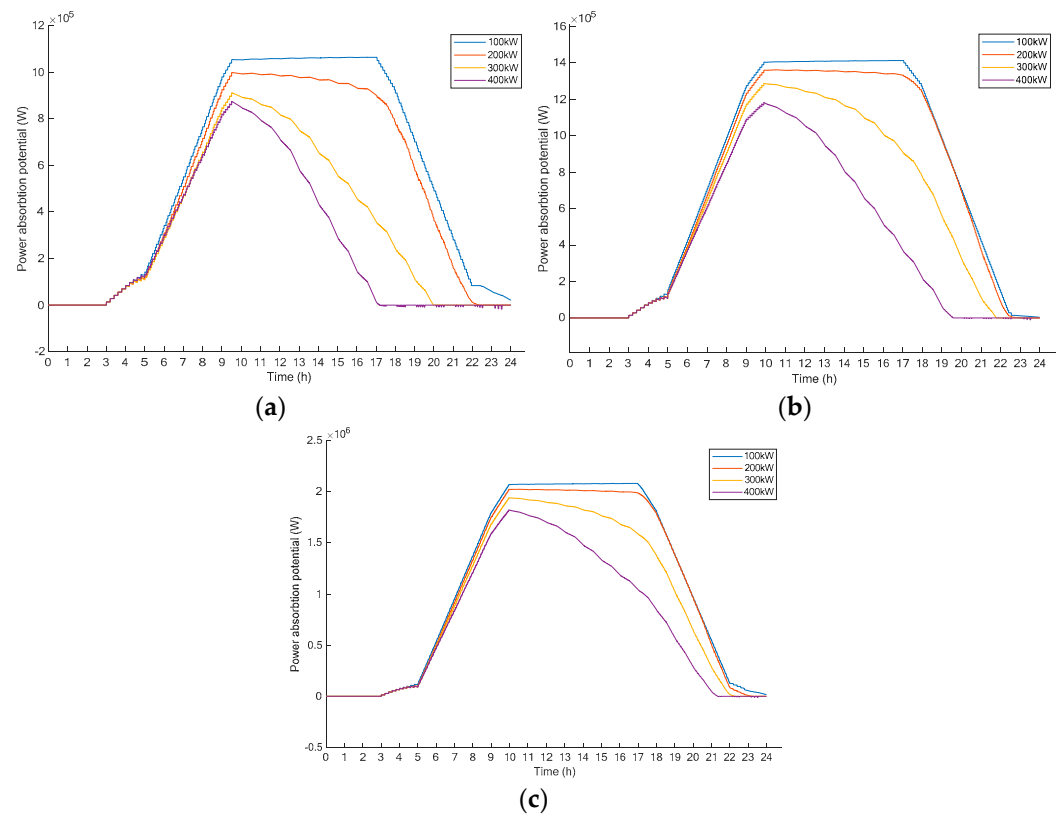


**Figure 9.** The total potential for power absorption with varying limits on grid connection for scenario 1 (20 kW)—(a) 75 EVs. (b) 100 EVs. (c) 150 EVs.

The optimum grid connection limits found for 75 EV is 100 kW and for 100/150 EVs is 200 kW.

**4.2. Scenario 2: Charging Rate 6 kW-AC Charger**

To explore this further, simulations were conducted to observe the system’s 24 h operation with different EV populations in three modes of 150, 100 and 75 EVs. The charging rate limit for each EV and the limit for grid connection were fixed at 6 kW and 200 kW, respectively. Figure 10 illustrates the potential collective power output of the V2G network across time. It is clear from the results that the maximum provision power output of all modes never reaches the global discharging limit of 6 kW. In other words, to be capable to integrate ERSs with AC slow charging station, it is required to have a higher number of EVs. This motivates the implementation of HESS, which will be evaluated in next scenario.

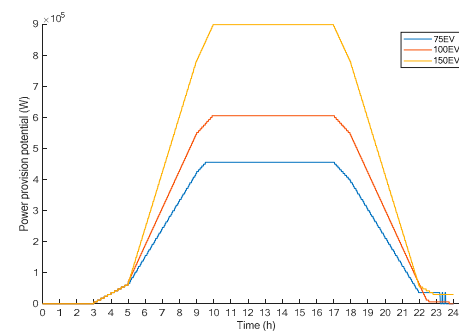


**Figure 10.** The total potential for power supply of trains with different numbers of EVs for scenario 2 (6 kW).

Figure 11 illustrates the capability of the EVCS for peak shaving of traction substation for 6 kW AC charging system. Considering the original power demands required by train traction substation during the busy hours of EVCS, the maximum peak power absorbed from the grid are found to be as 500, 350 and 200 kW for 75, 100 and 150 EVs. In other words, mode 3 with 150 EVs is suitable with 200 kW grid connection limit. However, considering morning hours and afternoon when EVs number are lower, the peak shaving purpose cannot occur. In other words, modes 1 and 2 cannot contain power demand at the grid connection, while in mode 3, the system has the possibility of peak shaving only at 9:00 in the morning up to 18:00.

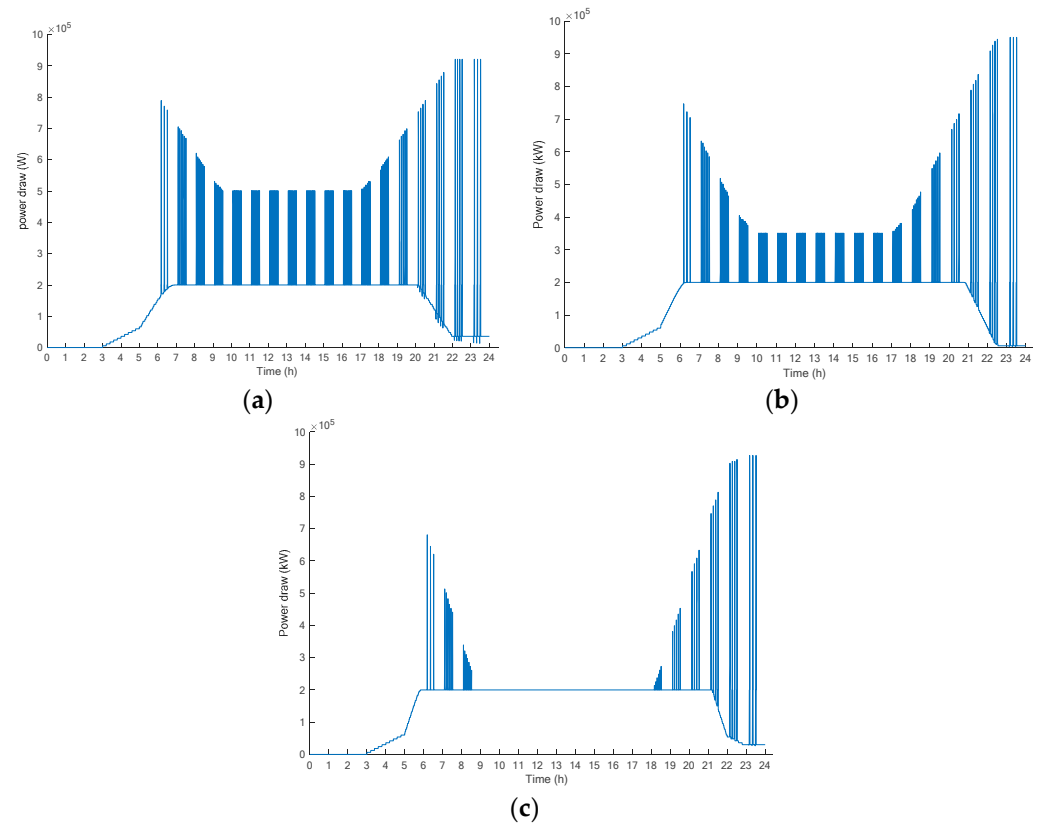


**Figure 11.** The amount of power consumed by the rail system from the substation and the power demands of the EV population with a connected V2G network over a 24 h (6 kW)—(a) 75 EVs. (b) 100 EVs. (c) 150 EVs.

The results related to the power absorption capability of EVs presented in Figure 12 show that with global charging limit of 6 kW, the threshold amount for regenerative braking power of trains cannot be provided for any of modes.

Only in mode 1 (up to 150 EVs), the system can absorb the maximum regenerative power, and this rate of power is around 60% of total regenerative power. In other words, all of the regenerated power cannot be accommodated in EVs batteries. This importance necessitates the existence of the energy sources.

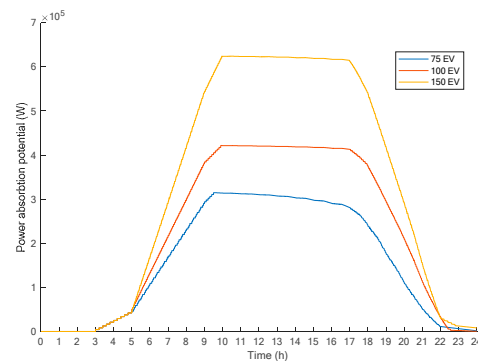


**Figure 12.** The total potential for power absorption of EV charging station with different numbers for scenario 2 (6 kW).

Figure 13 displays the progression of the state of charge (SOC) for the three EVs population with Table 3 providing the numerical amount for final SOC of each EV. In all three scenarios, there was a substantial increase in SOC for each control EV. However, the results show that the average increase in SOC during leaving for each EV is about 10%, which is not satisfactory and cannot encourage drivers to participate in V2G technology. Meanwhile, the results reveal that, for this scenario, the number of EVs in parking lot does not make significant changes in the SOC. As anticipated, since the grid connection limit remained constant at 200 kW for all modes (thereby restricting the amount of power that can be shared among EVs during smart charging intervals), the increase in SOC for each EV was greater for smaller populations of EVs.

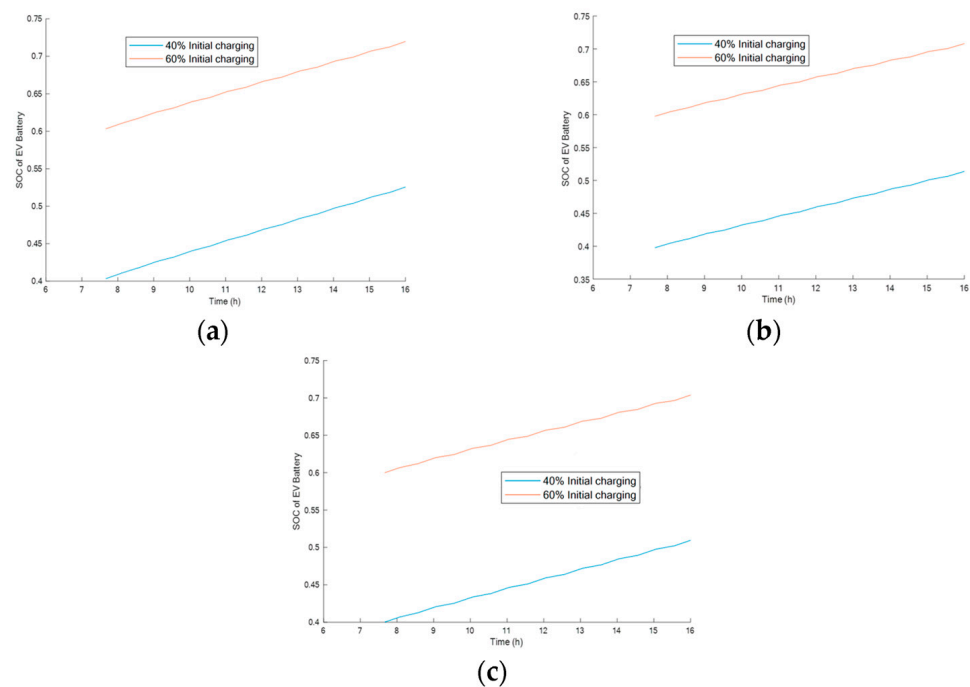


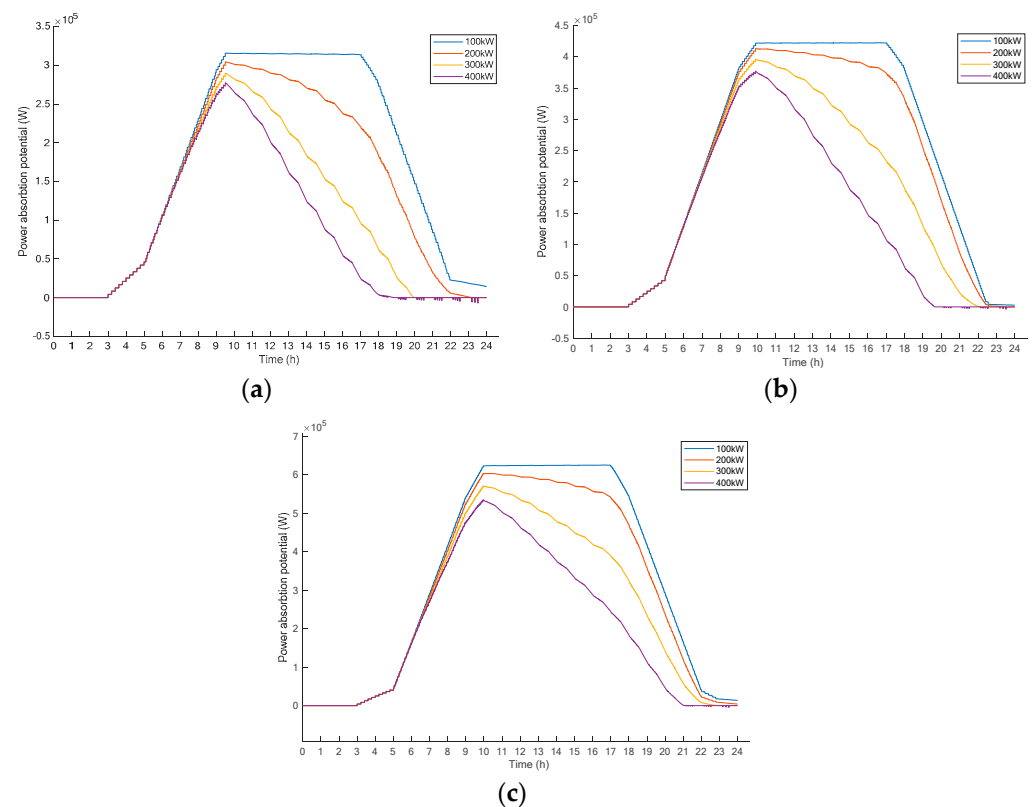
**Figure 13.** Variations in SOC in the three controlled EV groups of different numbers over time (6 kW)—(a) 75 EVs. (b) 100 EVs. (c) 150 EVs.

Comparing the results for charging rate 20 kW and 6 kW, it can be concluded that rate of SOC during the evaluation time is dependent on the number of EVs and charging rate. Whatever the charging rate decrease, the final SOC would be lower in comparison to the higher charging rate. The other factor that has influence on the SOC is the number of EVs. When the number of EVs increases, the share power for every EV decreases, and the final situation of the SOC is lower, and it takes more time for charging.

**Table 3.** The battery pack state of charge (SOC) of the control EVs with different EV population sizes for 6 kW scenario.

Initial Charge	Final Charge		
	75 EV	100 EV	150 EV
40%	52	51	49
60%	72	70	68

To analyze grid connection aspects, multiple simulations of 24 h system operation with different grid connection limits, ranging from 100 to 400 kW, is carried out for 6 kW scenario. The EV population size remained constant at 75, 100 and 150 EVs for all simulations. As depicted in Figure 14, when the grid connection limit is raised, the collective capacity of the EVs to draw power from the railway system is drastically reduced. This impact is more noticeable during the afternoon and evening periods as opposed to the early hours of the day because the number of active EVs in the park-and-ride area decrease. So, the share power would rise, and the vacant capacity of any EV battery would decrease dramatically. Therefore, in the evening, both the number of the active EVs and vacant capacity would decrease, so the capacity of the absorption regenerative power would dramatically decrease, and the trend of Figure 14 decrease in the evening and night. Increasing the grid connection power limit, the shared power and the rate of charging increase. So, batteries of EVs charge more quickly.

**Figure 14.** The total capability for power absorption with different limits on grid connection over 24-h—(a) 75 EVs. (b) 100 EVs. (c) 150 EVs.

Therefore, in the evening, the vacant capacity of the batteries dramatically decreases. Based on the results, it can be found that even with the optimum grid connection limit of 100 kW, the maximum power absorption potential for regenerative braking power of trains is 650 kW, which is almost 60% of the threshold.

#### 4.3. Scenario 3: Charging Rate 6 kW + HESS

Motivated by scenario 2, the importance of implementation of HESS emerged. Therefore, in scenario 3, the HESS is designed based on the requirements of scenario 2. Similar to the previous section, the primary factor that affects the effectiveness of the suggested V2G system is dependent on the size of the EV population that is linked to the system or the total number of EVs connected to it. To investigate this, a simulation was conducted using EV populations ranging from 75 up to 150 Evs, while maintaining a constant global charging rate limit for each EV and grid connection limit of 6 kW and 200 kW, respectively. Additionally, the system is equipped with a HESS to further optimize energy efficiency and absorb more regenerative braking energy.

Figure 15 depicts the power output potential of the V2G network at different time intervals in each of the three modes of EV populations. As the global discharging limit is set at 6 kW, which is lower than the maximum possible power output of the simulated Evs (none of the Evs are ever fully discharged), it is necessary to compensate the remaining power required as the traction power. Comparing Figures 10 and 15, it is clear that the total provision power for supplying trains and participating in V2G technologies has been increased significantly by almost 45%.

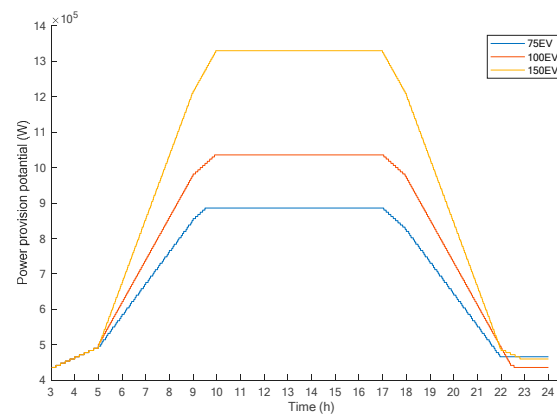
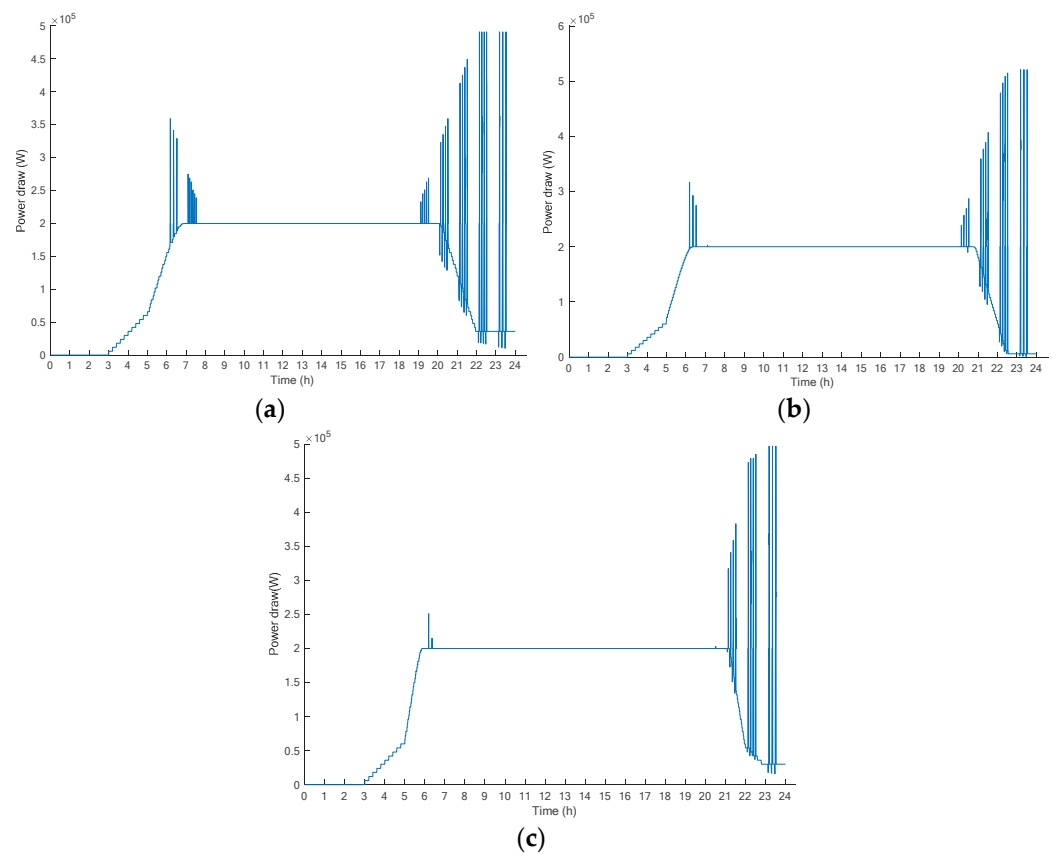


**Figure 15.** Total power provision potential of EV charging station for scenario 3 (6 kW + HESS).

The results in Figure 16 depict the capability of the EVCS for peak shaving of traction substation for 6 kW charging station with HESS. According to the results shown and considering the original power demands required by train traction substation during the busy hours of EVCS, the maximum peak power absorbed from the grid is found to be 200 kW for 75, 100 and 150 Evs. In comparison with the scenario 2, the performance of the scenario 3 is much better.

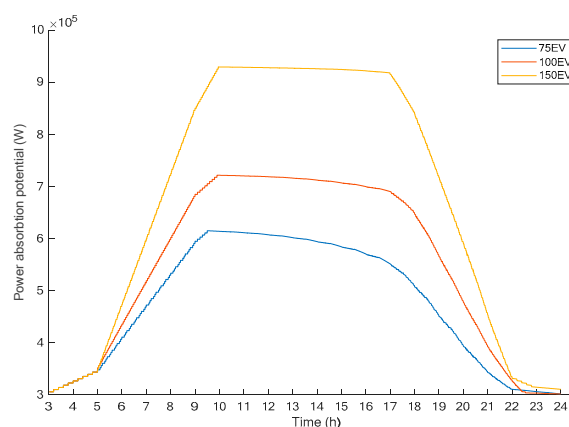
Unlike the previous scenario, scenario 3 has acceptable performance, and power demand from the grid, specially in the middle of the day, is confined to the grid connection (200 kW). Also, thanks to HESS, the power demand from the grid in the night has been reduced from 890 kW to 480 kW.

In other words, for all proposed EV populations, the integration scenario is compatible with the 200 kW grid connection limit. However, considering morning hours and afternoons when Evs number are lower, the peak shaving purpose cannot occur significantly. Results show that all modes have the possibility of peak shaving from 7:00 in the morning up to 19:00.



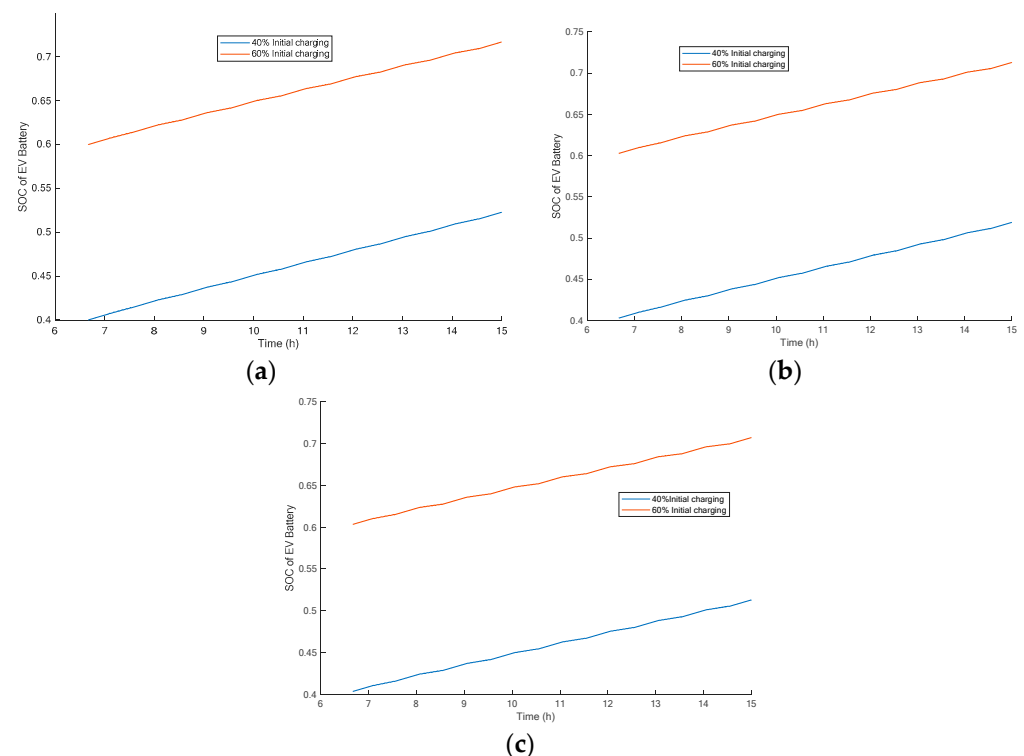
**Figure 16.** The amount of power consumed by the rail system from the substation and the power demands of the EV population with a connected V2G network over a 24 h (6 kW + HESS)—(a) 75 EVs. (b) 100 EVs. (c) 150 EVs.

The diagrams in Figure 16 display the V2G network’s ability to receive regenerative power during the day, which is determined by the maximum charging rate of all EVs at any given point (limited to a global charging limit of 6 kW plus HESS). Each EVs maximum charging power depends on its current state of charge (SOC) and may be much less than 6 kW. Similar to the previous method, number of active EVs has profound effect on the power absorption. Comparing Figures 12 and 17, it is clear that the total power absorption potential for supplying trains and participating in V2G technologies has been increased significantly by almost 38%.



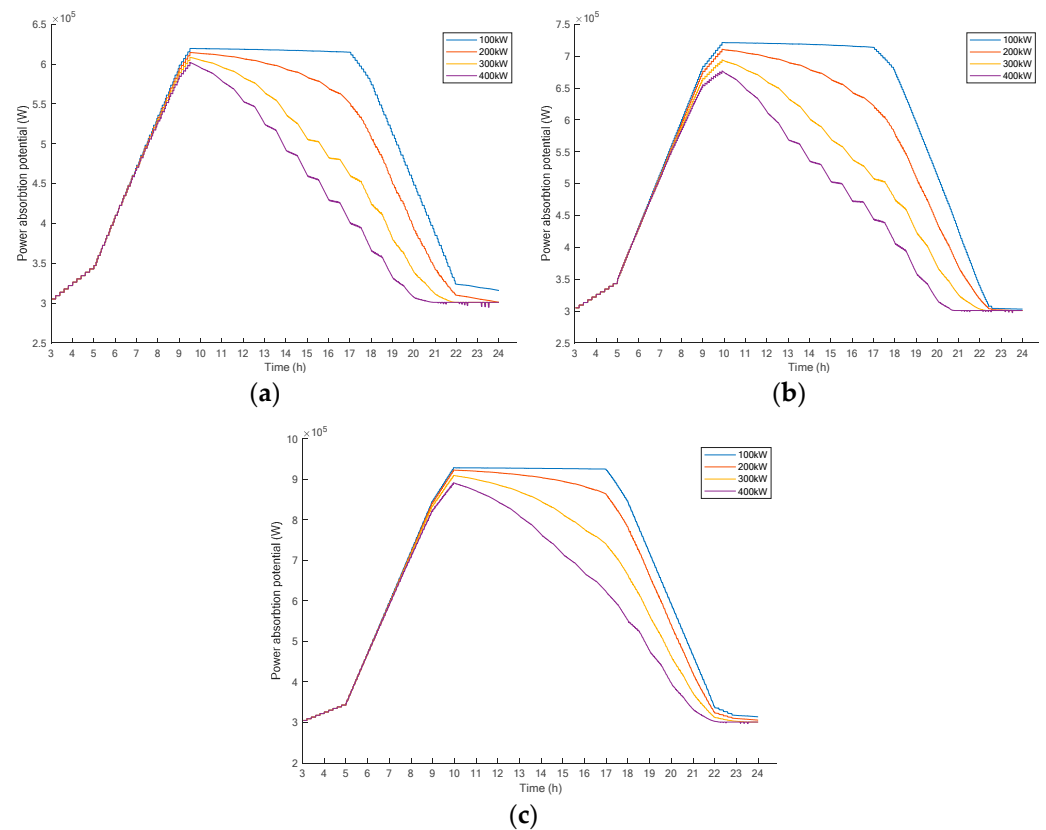
**Figure 17.** The total potential for power absorption of EV charging station with different numbers for scenario 3 (6 kW + HESS).

Figure 18 illustrates the progression of the state of charge for the three EV populations. Based on the results of figure, the maximum charging rate is considered 6 kW, and the charging rate is based on the SOC of the battery, which means the rate of absorption power has a relation with the SOC. Although the charging rate is low (6 kW) in comparison with 20 kW, the final position of the battery SOC is acceptable. The results show that the average increase in SOC during leaving for each EV is about 15%. Meanwhile, according to the results, the number of EVs in parking lot does not affect SOC scenario 1. In the proposed method, our first priority is to charge the EVs when the EVs are connected to the system and attempt to increase the SOC of every EV. So, in the first step, regenerative power is injected to EVs. Then, if there is regenerative power remaining, it is injected into the HESS. As anticipated, the increase in SOC per EV was greater for smaller populations of EVs as the grid connection limit remained fixed at 200 kW for all modes, limiting the amount of power that could be exchanged among EVs during intelligent charging intervals.



**Figure 18.** The variation in the state of charge (SOC) of the three designated control EVs with different sizes of EV populations (6 kW + HESS)—(a) 75 EVs. (b) 100 EVs. (c) 150 EVs.

As depicted in Figure 19, a higher grid connection limit has a notable negative impact on the capacity of the EV population to receive energy from the railway system. Similarly, two important factor have effect on the power absorption potential. The first factor is the grid connection power in which system absorbs power from the power network consciously. Therefore, whatever the grid connection power rise, the contribution of every EV in the grid connection would increase and the capacity for absorption of regenerative power would decrease. So, during the evening and night, the capacity of potential absorption dramatically decreases. Based on the results, it can be found that with the optimum grid connection limit of 100 kW, the maximum power absorption potential for regenerative braking power of trains is increased to 950 kW, which is almost 85% of the threshold.



**Figure 19.** The total capability for power absorption with different limits on grid connection over 24 h (6 kW + HESS)—(a) 75 EVs. (b) 100 EVs. (c) 150 EVs.

The results of the three scenarios are compared in terms of the four technical issues such as maximum provision power, maximum absorption power, maximum peak demand from the grid and minimum number of required EVs and is shown in Table 4. In the first scenario (20 kW), as the fast charging rate is considered, the maximum power provision is significantly high and is equal to 3000 kW for the 150 EV. In addition, even if number of EVs would be lower (75 EVs), there is no concern in providing the traction power for the acceleration mode. The second scenario (6 kW) cannot totally provide the traction power even in the case of maximum number of EVs (i.e., 150). But, in the modified scenario, which is third scenario, this problem is solved, and it can supply the traction power completely.

**Table 4.** Comparison between the results of the three scenarios.

Scenario	Charging Mode	Maximum Provision Power	Maximum Absorption Power	Maximum Peak Shaving	Minimum Number of Required EVs
1	20 kW	3000 kW	2000 kW	750 kW	75
2	6 kW	900 kW	620 kW	400 kW	200
3	6 kW + HESS	1350 kW	950 kW	700 kW	100

The maximum absorption power in the first scenario is 2000 kW, and it shows that the possibility for storing power is dramatically high, and we can completely absorb regenerative power. However, in the second scenario, with the maximum number of EVs, the system can only absorb 620 kW. For the third scenario, the maximum number of EVs in the proposed system can absorb about 950 kW, which is almost 85% of total regenerative power.

One of the important technical issues is the peak shaving power because the aim of the system mitigates the stress and tension in the power grid. Therefore, whenever the amount of peak shaving would be higher, the performance of the proposed system would be more reliable. With notice to this point, the first and third scenario (6 kW + HESS) exhibit the best performance in comparison with the other scenario. However, the main drawback of first scenario with DC fast charging system is a high cost of implementation in which at least 75 DC fast charger should be established in the station. It is not reasonable to implement such an expensive system.

Overall, the proposed HESS-based railway station integrated with EV charging station has the best performance in terms of four technical issues mentioned. In addition, the third scenario has lower cost of investment and lower cost of implementation in comparison to scenario 1.

## 5. Conclusions and Future Works

This paper proposed a sustainable transportation system model that is designed to increase energy efficiency and reduce costs of charging stations of EVs close to railway substations. The proposed model and power management unit transfer the braking energy of trains to EV charging station and charge the EVs. Meanwhile, the possibility of the proposed system in participating as a V2G technology and utilizing EV batteries to provide auxiliary support to trains during acceleration mode is investigated along with considering peak shaving objectives. In order to solve the incompatibility of power ranges, three different scenarios are evaluated including DC fast charging station, AC low charging station and collaborative hybrid energy storage based AC charging station as EV charging station type. The results are studied for different EV population numbers, charging rates and contractual power grids. Park-and-ride data of an area in Milan San Donato metro substation was used as a case study. The simulation results confirmed that the proposed interconnected system works well with a higher number of EVs parked in the station, but the system's performance is significantly affected by the low number of EVs during the morning and late hours of the evening. The maximum absorption power in the first scenario with DC fast chargers showed that the possibility for storing the regenerative power is dramatically high, while in the second scenario with AC chargers, even with the maximum number of EVs, the system cannot absorb the whole regenerative power. Accordingly, as the main idea of the paper, scenario 3 is studied that takes advantage of HESS. Based on results, it is revealed that the maximum number of EVs in the proposed system can absorb almost 85% of total regenerative power.

Overall, the proposed HESS-based railway station integrated with EV charging station has the best performance in terms of four technical issues, i.e., maximum provision power, maximum absorption power, maximum peak demand from the grid and minimum number of required EVs. In addition, the third scenario has lower cost of investment and lower cost of implementation in comparison to scenario 1. Accordingly, with the proper designing of EV charging station in park-and-ride regions, the proposed system has the potential to significantly reduce peak energy demand in highly demanding transportation systems and to increase their efficiency by charging EV batteries using regenerative energy of trains.

There are several key areas to focus on for the further development of our study. Firstly, incorporating the stochastic behavior of EV batteries is crucial to capture the inherent variability in SOC levels and charging patterns among EVs. This will provide a more realistic representation of real-world scenarios and yield more accurate and robust results. Secondly, exploring the application of an AI-based energy management system can optimize energy flow, load balancing and charging schedules. By leveraging machine learning and optimization algorithms, intelligent decision-making can be achieved, leading to improved efficiency and performance of the integrated system. Additionally, considering the impact of power charging profiles for DC fast charging systems on the proposed model will offer insights into system dynamics and facilitate the development of tailored charging strategies. Lastly, designing a prediction method based on historical data and relevant

factors can anticipate future charging demands, enabling proactive planning and resource allocation. By addressing these aspects, our study can advance the understanding and practical implementation of the integrated EV charging system.

**Author Contributions:** In preparation of this paper, H.J.K. and M.G. conducted the methodology, data curation, software-based simulations and writing—original draft, and M.B. and D.Z. conducted the validation, visualization and the resources and funding acquisition along with the editing and supervision; All authors have read and agreed to the published version of the manuscript.

**Funding:** This research received no external funding.

**Data Availability Statement:** No additional data is available to report.

**Conflicts of Interest:** The authors declare no conflict of interest.

## Nomenclature

### Acronyms

<b>AC</b>	Alternative current
<b>CW</b>	Charging weight
<b>DC</b>	Direct current
<b>DCW</b>	Discharging weight
<b>ERS</b>	Electric railway system
<b>ESS</b>	Energy storage System
<b>EV</b>	Electric vehicle
<b>EVCI</b>	Electric vehicle charging infrastructure
<b>EVCS</b>	Electric vehicle charging station
<b>G2V</b>	Grid to vehicle
<b>HESS</b>	Hybrid energy storage system
<b>IEA</b>	International energy agency
<b>RBE</b>	Regenerative braking energy
<b>RES</b>	Renewable energy source
<b>SOC</b>	State of the charge
<b>TSS</b>	Traction substation
<b>V2G</b>	Vehicle to grid

## References

- International Energy Agency. *Global EV Outlook 2019*; IEA Publications: Paris, France, 2019; pp. 9–10. Available online: <https://www.iea.org/reports/global-ev-outlook-2019> (accessed on 3 February 2023).
- Longo, M.; Foadelli, F.; Yaïci, W. Electric vehicles integrated with renewable energy sources for sustainable mobility. *New Trends Electr. Veh. Powertrains* **2018**, *10*, 203–223.
- Kaleybar, H.J.; Brenna, M.; Castelli-Dezza, F.; Zaninelli, D. Sustainable MVDC Railway System Integrated with Renewable Energy Sources and EV Charging Station. In Proceedings of the 2022 IEEE Vehicle Power and Propulsion Conference (VPPC), Merced, CA, USA, 1–4 November 2022; IEEE: New York, NY, USA, 2022; pp. 1–6.
- Richardson, D.B. Electric vehicles and the electric grid: A review of modeling approaches, Impacts, and renewable energy integration. *Renew. Sustain. Energy Rev.* **2013**, *19*, 247–254. [[CrossRef](#)]
- Colombo, C.G.; Miraftebzadeh, S.M.; Saldarini, A.; Longo, M.; Brenna, M.; Yaici, W. Literature Review on Wireless Charging Technologies: Future Trend for Electric Vehicle? In Proceedings of the 2022 IEEE Second International Conference on Sustainable Mobility Applications, Renewables and Technology (SMART), Cassino, Italy, 23–25 November 2022; pp. 1–5.
- Khodaparastan, M.; Mohamed, A.A.; Brandauer, W. Recuperation of regenerative braking energy in electric rail transit systems. *IEEE Trans. Intell. Transp. Syst.* **2019**, *20*, 2831–2847. [[CrossRef](#)]
- González-Gil, A.; Palacin, R.; Batty, P. Sustainable urban rail systems: Strategies and technologies for optimal management of regenerative braking energy. *Energy Convers. Manag.* **2013**, *75*, 374–388. [[CrossRef](#)]
- Jiang, Y.; Liu, J.; Tian, W.; Shahidepour, M.; Krishnamurthy, M. Energy Harvesting for the Electrification of Railway Stations: Getting a charge from the regenerative braking of trains. *IEEE Electr. Mag.* **2014**, *2*, 39–48. [[CrossRef](#)]
- Lu, S.; Weston, P.; Hillmans, S.; Gooi, H.B.; Roberts, C. Increasing the regenerative braking energy for railway vehicles. *IEEE Trans. Intell. Transp. Syst.* **2014**, *15*, 2506–2515. [[CrossRef](#)]
- Hernandez, J.C.; Sutil, F.S. Electric vehicle charging stations fed by renewable: PV and train regenerative braking. *IEEE Lat. Am. Trans.* **2016**, *14*, 3262–3269. [[CrossRef](#)]

11. Falvo, M.C.; Lamedica, R.; Bartoni, R.; Maranzano, G. Energy management in metro-transit systems: An innovative proposal toward an integrated and sustainable urban mobility system including plug-in electric vehicles. *Electr. Power Syst. Res.* **2011**, *81*, 2127–2138. [[CrossRef](#)]
12. Şengör, İ.; Kılıçkiran, H.C.; Akdemir, H.; Kekezoğlu, B.; Erdinc, O.; Catalao, J.P. Energy management of a smart railway station considering regenerative braking and stochastic behaviour of ESS and PV generation. *IEEE Trans. Sustain. Energy* **2017**, *9*, 1041–1050. [[CrossRef](#)]
13. Akbari, S.; Hashemi-Dezaki, H.; Fazel, S.S. Optimal clustering-based operation of smart railway stations considering uncertainties of renewable energy sources and regenerative braking energies. *Electr. Power Syst. Res.* **2022**, *213*, 108744. [[CrossRef](#)]
14. Brenna, M.; Foadelli, F.; Kaleybar, H.J. The Evolution of Railway Power Supply Systems Toward Smart Microgrids: The concept of the energy hub and integration of distributed energy resources. *IEEE Electr. Mag.* **2020**, *8*, 12–23. [[CrossRef](#)]
15. Jafari Kaleybar, H.; Brenna, M.; Foadelli, F.; Castelli Dezza, F. Sustainable Electrified Transportation Systems Integration of EV and E-bus Charging Infrastructures to Electric Railway Systems. In *Electric Transportation Systems in Smart Power Grids*; CRC Press: Boca Raton, FL, USA, 2023; pp. 237–267.
16. Krueger, H.; Fletcher, D.; Cruden, A. Vehicle-to-Grid (V2G) as line-side energy storage for support of DC-powered electric railway systems. *J. Rail Transp. Plan. Manag.* **2021**, *19*, 100263. [[CrossRef](#)]
17. Kaleybar, H.J.; Brenna, M.; Foadelli, F. EV charging station integrated with electric railway system powering by train regenerative braking energy. In Proceedings of the 2020 IEEE Vehicle Power and Propulsion Conference (VPPC), Virtual Conference, 18 November–16 December 2020; pp. 1–6.
18. Ahmadi, M.; Jafari Kaleybar, H.; Brenna, M.; Castelli-Dezza, F.; Carmeli, M.S. Integration of Distributed Energy Resources and EV Fast-Charging Infrastructure in High-Speed Railway Systems. *Electronics* **2021**, *10*, 2555. [[CrossRef](#)]
19. Golnargesi, M.; Kaleybar, H.J.; Brenna, M.; Zaninelli, D. Collaborative Electric Vehicle Charging Strategy with Regenerative Braking Energy of Railway Systems in Park & Ride Areas. In Proceedings of the 14th Power Electronics, Drive Systems, and Technologies Conference (PEDSTC), Tehran, Iran, 31 January–2 February 2023; pp. 1–5.
20. Bae, C.H. A simulation study of installation locations and capacity of regenerative absorption inverters in DC 1500 V electric railways system. *Simul. Model. Pract. Theory* **2009**, *17*, 829–838. [[CrossRef](#)]
21. Ghaviha, N.; Campillo, J.; Bohlin, M.; Dahlquist, E. Review of application of energy storage devices in railway transportation. *Energy Procedia* **2017**, *105*, 4561–4568. [[CrossRef](#)]
22. Ladimir, P.; Iurii, P. Supercapacitor Energy Storages in Hybrid Power Supplies for Frequency-Controlled Electric Drives: Review of Topologies and Automatic Control Systems. *Energies* **2023**, *16*, 3287. [[CrossRef](#)]
23. Arbolea, P.; El-Sayed, I.; Mohamed, B.; Mayet, C. Modeling, Simulation and Analysis of On-Board Hybrid Energy Storage Systems for Railway Applications. *Energies* **2019**, *12*, 2199. [[CrossRef](#)]
24. Qu, K.; Yuan, J. Optimization research on hybrid energy storage system of high-speed railway. *IET Gener. Transm. Distrib.* **2021**, *15*, 2835–2846. [[CrossRef](#)]

**Disclaimer/Publisher’s Note:** The statements, opinions and data contained in all publications are solely those of the individual author(s) and contributor(s) and not of MDPI and/or the editor(s). MDPI and/or the editor(s) disclaim responsibility for any injury to people or property resulting from any ideas, methods, instructions or products referred to in the content.